

The A -Scaling of the Multiplicity Distributions of π^- , K^- and \bar{P} Interactions with Nuclei at 40 GeV/c

RISK Collaboration

A.M. Mosienko

Institute for High Energy Physics, SU-480082 Alma-Ata, USSR

U. Gensch, T. Naumann, C. Spiering

Institute for High Energy Physics, DDR-Berlin, GDR

L. Diósi, T. Gemesy, L. Jenik, J. Krasnovsky, Gy. Pintér, I. Wagner

Central Research Institute for Physics, H-1525 Budapest, Hungary

A.V. Bannikov, J. Bohm, Ja.V. Grishkevich, Z.V. Krumstein, Yu.P. Merekov, V.I. Petrukhin, K. Piska, K. Safarik, J. Sedlak, G.A. Shelkov, L.G. Tkachev, L.S. Vertogradov

Joint Institute for Nuclear Research, SU-141980 Dubna, USSR

T. Soukup, A. Valkarova, S. Valkar, P. Zavada

Institute of Physics CSASc and Nuclear Centre of Charles University, CS-18000 Prague, Czechoslovakia

V.N. Penev

Institute for Nuclear Research and Nuclear Energy, Sofie, Bulgaria

E.Sh. Ioramishvili, A.K. Javrishvili, A.I. Kharchilava, T.A. Lomtadze, E.S. Mailian, A.A. Rasdolskaja, L.B. Shalamberidze

Institute of Physics of the Academy of Science of Georgian SSR, SU-380086 Tbilisi, USSR

J. Gajewski, J.A. Zakrzewski

Institute of Experimental Physics Warsaw University, PL-00681 Warsaw, Poland

Received 29 July 1985; in revised form 25 November 1985

Abstract. The multiplicity distributions of charged particles produced from π^- , K^- and \bar{p} interactions with the nuclei Li, C, S, Cu, CsI, Pb at 40 GeV/c were studied. It was found that the linear relation $D = a\langle n \rangle + b$ is satisfied for the distributions of different kinds of secondary particles including knocked out protons. Consequently, the use of the scaling variable $z' = (an + b)/(a\langle n \rangle + b)$ ensures the scaling of the distributions with respect to the mass number A at least up to the second moment.

1. Introduction

The nature of the KNO-scaling [1] for the multiplicity distributions at high energies and the possibility of its violation are of great interest for the dynamics of strong interactions. In fact the KNO-scaling has been verified for all hadron-proton inelastic processes at $50 \lesssim p_{\text{LAB}} \lesssim 300$ GeV/c [2], but the recent data from the SPS-collider [3] have shown its violation.

A number of formulae [4, 5] depending on other scaling variables than the usual $z=n/\langle n \rangle$ has been proposed for the description of the “universal” shape of a multiplicity distribution in hadron-hadron interactions. One of them is the scaling variable:

$$z' = \frac{an+b}{a\langle n \rangle + b}. \quad (1)$$

This variable can be deduced from the empirical relation between the mean value and the dispersion of the multiplicity distribution:

$$D = a\langle n \rangle + b, \quad D = \sqrt{\langle n^2 \rangle - \langle n \rangle^2} \quad (2)$$

which was studied for pp collisions by Wróblewski [6]. It was shown that if one uses variable (1), scaling of the multiplicity distribution holds even for lower energies, $p_{\text{LAB}} \gtrsim 12$ GeV/c.

Some recent experiments on hadron-nucleus interactions (π^- Ne at 50 GeV/c [7], π^- C at 40 GeV/c [8], p Ar, p Xe, \bar{p} Ar, \bar{p} Xe at 200 GeV/c [9] and our data on collisions of π^- , K^- , \bar{p} with nuclei ($7 \leq A \leq 207$) at 40 GeV/c [10]) have shown, that for

the studied nuclei the distribution $\langle n \rangle \frac{\sigma_n}{\sigma_{\text{inel}}} = \psi(z)$ of negatively charged particles has within the statistical errors the same shape as that in hadron-proton collisions [11].

On the other hand the analysis of $\pi^- A$ data from the electronic experiment [12] (without charge identification) has shown, that the relation (2) holds for the multiplicity distribution of relativistic particles (“shower” particles) in the sense, that the same line is populated not only by values corresponding to different primary energies but also to different nuclear targets ($12 \leq A \leq 238$, $p_{\text{LAB}} = 100, 175$ GeV/c). In addition, the corresponding parameters of curve (2) practically coincide with those in hadron-proton interactions.

However, for a sensitive test of KNO scaling and relation (2) in the case of hadron-nucleus interactions more experimental results are needed. Especially, new data on π^\pm , K^\pm , p , \bar{p} interactions on “pure” nuclear targets and with charge identification of secondary particles are required.

In our experiment, targets made from Li, C, Si, Cu, CsI and Pb were mounted in the streamer chamber RISK. These nuclear targets were exposed to a 40 GeV/c $\pi^-/K^-/\bar{p}$ -beam of the Serpukhov PS. In this paper, we analyze the multiplicity distributions of different kinds of secondary particles. The aim is to check the validity of relation (2) and the scaling in z' (1). Our study concerns the test of scaling with respect to mass number A since we have only one value of primary energy but a broad region of nuclear targets.

2. Experimental Procedure

The experimental set-up of the spectrometer RISK and the method of analysis were described elsewhere [10, 13, 14].

In our experiment we can identify the charge of secondary particles. In the case of “slow” particles ($p_{\text{LAB}} \lesssim 500$ MeV/c) we can identify protons according to their ionization. Besides, using special templates, we determined the number of charged particles with momenta below ≈ 500 MeV/c.

During the scanning procedure events corresponding to 0 and 1 prong were excluded. The resulting event sample contains 2,138 $\pi^- A$, 2,456 $K^- A$ and 7,011 $\bar{p} A$ interactions. Most of the contribution of coherent events in the 3-prong sample was not rejected by the trigger. These events ($\sim 2\%$ of all) have been excluded by subtraction of the excess visible at $n_{\text{ch}}=3$ in the multiplicity distribution of events with only fast tracks ($p_{\text{LAB}} \gtrsim 500$ MeV/c).

We have used thin targets ($\sim 1\%$ of absorption length), but still protons of momenta below ≈ 100 –180 MeV/c are mostly stopped in them, as we have found by Monte-Carlo calculation. Heavy nuclear fragments have little chance of leaving the targets, so we have a rather good identification of knocked out protons in the momentum interval 180 to 500 MeV/c.

Our analysis concerns the following multiplicities:

- 1) n_{ch} – all charged particles,
- 2) n^\pm – all positively/negatively charged particles,
- 3) n_p – slow protons in the momentum interval 180–500 MeV/c,
- 4) $n_{\text{FAST}} = n_{\text{ch}} - n_p$ – charged particles with the exclusion of slow protons,
- 5) $n_{\text{FAST}}^\pm = n^\pm - n_p$ – positively charged particles with exclusion of slow protons,
- 6) $Q = n^+ - n^- + 1$ – net charge.

The mean multiplicities and the dispersion of all charged particles have been corrected with respect to:

- 1) Dalitz pair production and γ -conversion inside the targets;
- 2) secondary interactions inside the targets;
- 3) V^0 -decays within the targets.

The sum of these corrections amounts to $\sim 4\%$ for Li and $\sim 11\%$ for Pb.

3. Experimental Results

1. Dependence of D on $\langle n \rangle$

In Figs. 1–6 the dependences of the dispersions on the mean values for n_{ch} , n_{FAST} , n_{FAST}^\pm , n^\pm and n_p are

shown. The data corresponding to n^\pm and n_p are listed in Tables 1, 2. We observe that the linear dependence (2) is well-obeyed by all the types of multiplicities. Beside that, within statistical errors the same dependence holds for different projectile par-

ticles. The results of the fit $D = a\langle n \rangle + b$ are listed in Table 3. The mean number of all knocked out protons can be estimated from the average net charge:

$$\langle Q \rangle = \langle n^+ \rangle - \langle n^- \rangle + 1. \tag{3}$$

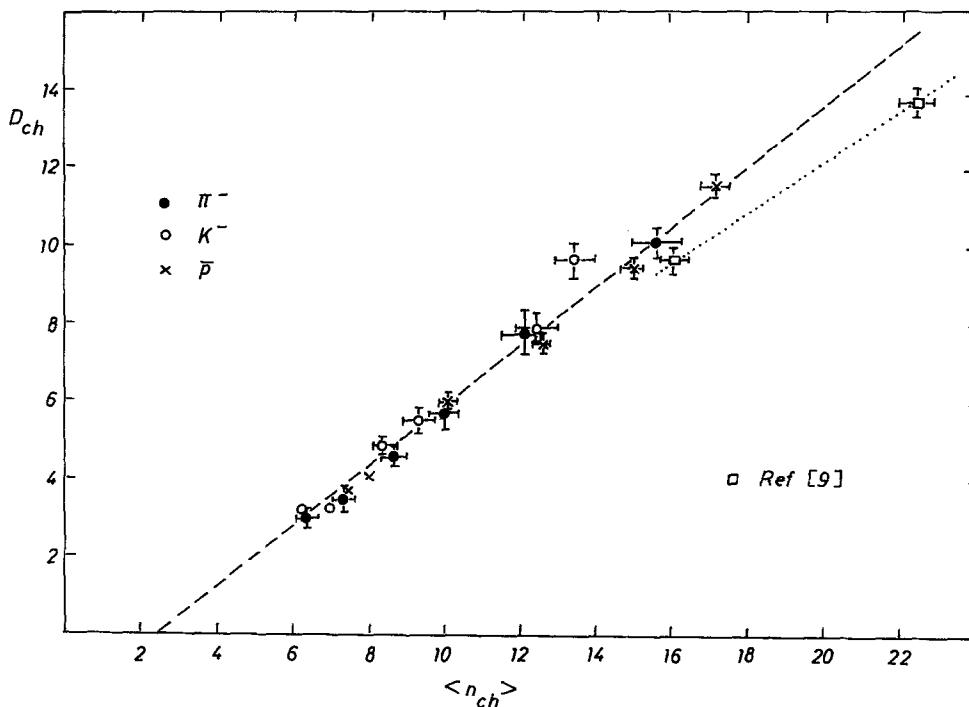


Fig. 1. Dispersion of the multiplicity distribution of all charged secondary particles as a function of the mean multiplicity. The dashed line is the fit $D_{ch} = 0.78\langle n_{ch} \rangle - 2.01$ and the dotted line is taken from experiment [9]

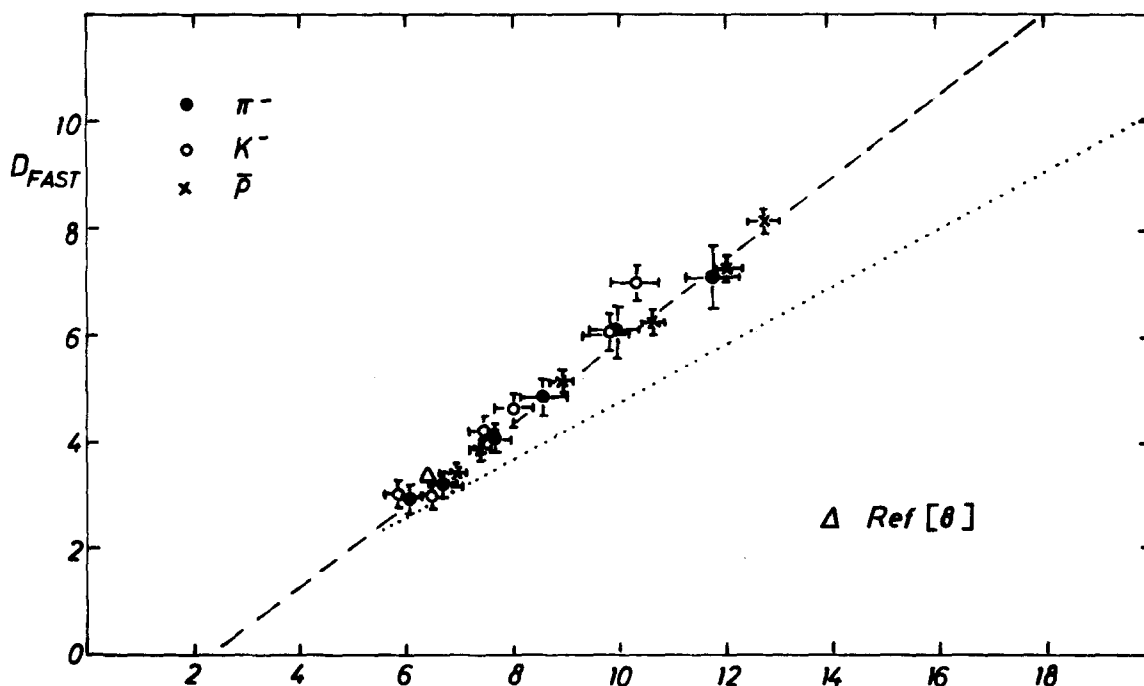


Fig. 2. Dispersion of the multiplicity distribution of charged secondary particles without identified protons as a function of the mean multiplicity. The dashed line is the fit $D_{FAST} = 0.75\langle n_{FAST} \rangle - 1.62$ and the dotted line $D = 0.54\langle n \rangle - 0.59$ is taken from experiment [12]

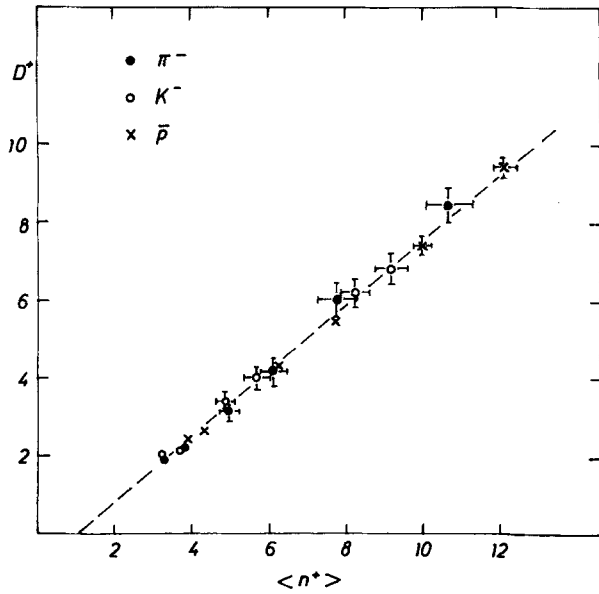


Fig. 3. Dispersion of the multiplicity distribution of all positively charged secondary particles as a function of the mean multiplicity. The dashed line is the fit $D^+ = 0.83 \langle n^+ \rangle - 0.85$

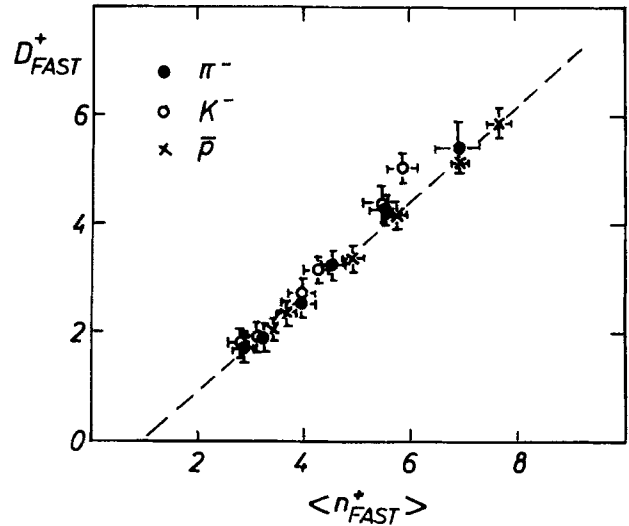


Fig. 4. Dispersion of the multiplicity distribution of all positively charged secondary particles without identified protons as a function of the mean multiplicity. The dashed line is the fit $D_{FAST}^+ = 0.84 \langle n_{FAST}^+ \rangle - 0.69$

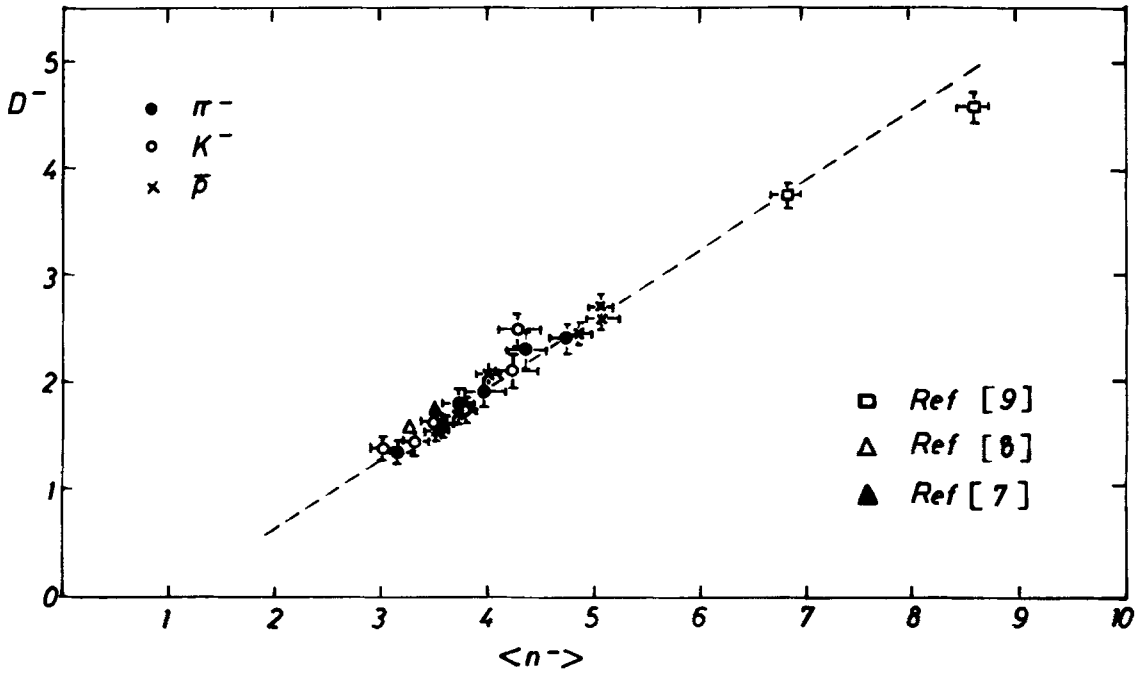


Fig. 5. Dispersion of the multiplicity distribution of all negatively charged secondary particles as a function of the mean multiplicity. The dashed line is the fit $D^- = 0.64 \langle n^- \rangle - 0.60$

Let us note, that one can expect the dispersion D_Q to be somewhat larger than that of really knocked out protons, because the difference $n^+ - n^-$ can be enhanced by charge exchange processes inside the nucleus:



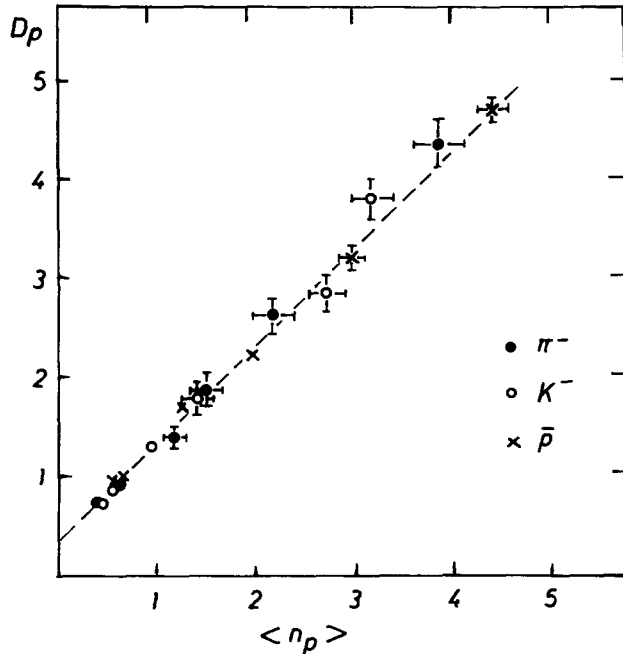
In the result, the net charge can be even negative [15]. On the other hand, the effects of exchange processes (4a), (4b) could mutually cancel with respect to the average number of all knocked out protons. The dependence D_Q on $\langle Q \rangle$ is shown in

Table 1. The mean multiplicities of all positively/negatively charged particles and identified protons ($p_{\text{LAB}} \lesssim 500$ MeV/c) for $\pi^- A$, $K^- A$ and $\bar{p} A$ collisions

A	$\pi^- A$	$K^- A$	$\bar{p} A$
$\langle n^+ \rangle$			
Li	3.26 ± 0.10	3.24 ± 0.10	3.92 ± 0.10
C	3.79 ± 0.15	3.76 ± 0.15	4.32 ± 0.10
S	5.00 ± 0.20	4.93 ± 0.20	6.20 ± 0.15
Cu	6.03 ± 0.35	5.71 ± 0.30	7.80 ± 0.15
CaI	7.90 ± 0.50	8.23 ± 0.40	10.05 ± 0.25
Pb	10.73 ± 0.55	9.20 ± 0.40	12.18 ± 0.30
$\langle n^- \rangle$			
Li	3.17 ± 0.10	3.02 ± 0.10	3.51 ± 0.05
C	3.53 ± 0.10	3.33 ± 0.10	3.72 ± 0.10
S	3.75 ± 0.10	3.53 ± 0.10	4.06 ± 0.10
Cu	4.04 ± 0.20	3.75 ± 0.15	4.96 ± 0.10
CsI	4.56 ± 0.20	4.31 ± 0.20	5.15 ± 0.15
Pb	4.87 ± 0.20	4.36 ± 0.20	5.21 ± 0.15
$\langle n_p \rangle$			
Li	0.38 ± 0.05	0.45 ± 0.05	0.56 ± 0.04
C	0.61 ± 0.05	0.54 ± 0.05	0.65 ± 0.04
S	1.02 ± 0.10	0.96 ± 0.08	1.24 ± 0.06
Cu	1.46 ± 0.15	1.39 ± 0.12	1.97 ± 0.07
CsI	2.15 ± 0.20	2.68 ± 0.20	2.95 ± 0.11
Pb	3.83 ± 0.28	3.14 ± 0.20	4.42 ± 0.15

Table 2. The dispersions of the multiplicity distributions of all positively/negatively charged particles and identified protons ($p_{\text{LAB}} \lesssim 500$ MeV/c) for $\pi^- A$, $K^- A$ and $\bar{p} A$ collisions

A	$\pi^- A$	$K^- A$	$\bar{p} A$
D^+			
Li	1.90 ± 0.10	2.05 ± 0.10	2.43 ± 0.10
C	2.22 ± 0.10	2.19 ± 0.15	2.59 ± 0.10
S	3.16 ± 0.15	3.41 ± 0.15	4.30 ± 0.15
Cu	4.22 ± 0.30	4.09 ± 0.20	5.48 ± 0.15
CsI	6.14 ± 0.45	6.18 ± 0.35	7.42 ± 0.15
Pb	8.50 ± 0.45	6.89 ± 0.35	9.45 ± 0.20
D^-			
Li	1.37 ± 0.06	1.42 ± 0.05	1.64 ± 0.05
C	1.59 ± 0.06	1.46 ± 0.06	1.77 ± 0.06
S	1.81 ± 0.10	1.75 ± 0.06	2.13 ± 0.06
Cu	1.95 ± 0.15	1.86 ± 0.10	2.53 ± 0.06
CsI	2.50 ± 0.20	2.22 ± 0.15	2.68 ± 0.10
Pb	2.53 ± 0.20	2.58 ± 0.15	2.80 ± 0.10
D_p			
Li	0.73 ± 0.08	0.75 ± 0.06	0.97 ± 0.08
C	0.95 ± 0.06	0.87 ± 0.06	0.99 ± 0.06
S	1.39 ± 0.08	1.30 ± 0.06	1.71 ± 0.13
Cu	1.87 ± 0.17	1.79 ± 0.14	2.18 ± 0.07
CsI	2.64 ± 0.20	2.83 ± 0.18	3.18 ± 0.09
Pb	4.36 ± 0.24	3.91 ± 0.21	4.68 ± 0.12

**Fig. 6.** Dispersion of the multiplicity distribution of all identified protons ($p_{\text{LAB}} \lesssim 500$ MeV/c) as a function of the mean multiplicity. The dashed line is the fit $D_p = 0.98 \langle n_p \rangle + 0.35$ **Fig. 7.** Again linear form holds independently of the primary particle.

We can compare our results with the bubble chamber data on $\pi^- C$ at 40 GeV/c [8], $\pi^- Ne$ at

Table 3. The results of the linear fit of the dependence of dispersion on mean value for different multiplicity distributions. The table demonstrates the correlation between the slopes of the lines and the average relative amount of knocked out protons; see text

	a	b	χ^2/NDF	$(r_{\text{Li}} + r_{\text{Pb}})/2$
n^-	0.64 ± 0.04	-0.60 ± 0.16	23/16	0
n_{FAST}^-	0.75 ± 0.03	-1.62 ± 0.32	40/16	0.20
n_{ch}^-	0.78 ± 0.03	-2.01 ± 0.25	33/16	0.33
n_{FAST}^+	0.84 ± 0.03	-0.69 ± 0.17	21/16	0.36
n^+	0.83 ± 0.02	-0.85 ± 0.16	15/16	0.51
Q	0.94 ± 0.03	0.24 ± 0.07	23/16	1
n_p	0.98 ± 0.05	0.35 ± 0.04	14/16	1

50 GeV/c [7], the streamer chamber data on $\bar{p} Ar$, $\bar{p} Xe$ at 200 GeV/c [9] and those from the electronic experiment [12] on $\pi^- A$ interactions at 100 and 175 GeV/c.

Our result concerning the dependence D^- on $\langle n^- \rangle$ (see Fig. 5) is consistent with the available data at our and an adjacent energy (50 GeV). Moreover the extrapolation of our line also meets the data at 200 GeV/c.

The good agreement between our and the propan chamber data [8] is apparent in Fig. 2 where D and $\langle n \rangle$ of the multiplicities of charged particles without identified protons are shown (in the propan chamber the protons are identified in the momentum interval $140 \div 750$ MeV/c).

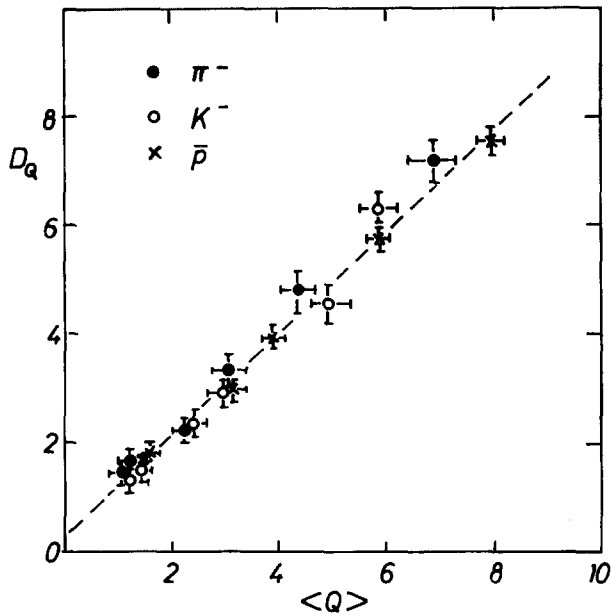


Fig. 7. Dispersion of the multiplicity distribution of the net charge $Q = n^+ - n^- + 1$ as a function of the mean multiplicity. The dashed line is the fit $D_Q = 0.94\langle Q \rangle + 0.24$

On the other hand, the same figure shows a discrepancy between our fit and that from the electronic experiment [12] in which only “shower” particles with velocity $\beta = v/c \geq 0.85$ have been registered. In Fig. 1, a similar discrepancy is apparent between our dependence $D_{ch} = a\langle n_{ch} \rangle + b$ and the data from the streamer chamber experiment [9] at 200 GeV/c.

Since the quantity $\langle Q \rangle$ measures the mean number of all knocked out protons, the difference $\langle Q_{FAST} \rangle = \langle Q \rangle - \langle n_p \rangle$ gives the mean number of the protons with the momenta above ≈ 500 MeV/c. Therefore the relative admixture of the protons in the multiplicities n_{ch} , n^+ , n_{FAST} , n_{FAST}^+ on a given target can be appreciated by the ratios:

$$r_A = \frac{\langle Q \rangle}{\langle n_{ch} \rangle}, \frac{\langle Q \rangle}{\langle n^+ \rangle}, \frac{\langle Q_{FAST} \rangle}{\langle n_{FAST} \rangle}, \frac{\langle Q_{FAST} \rangle}{\langle n_{FAST}^+ \rangle}.$$

Table 3 demonstrates the correlation between the slopes of the lines and the relative amount of knocked-out protons in the corresponding multiplicity. The values of the ratios listed in the last column are obtained as the average of those corresponding to our lightest (Li) and heaviest (Pb) nuclear targets. (We have put $r_A = 1$ for n_p , Q since they measure the protons exclusively and on contrary negatively charged particles do not contain any protons so $r_A = 0$.)

The slope corresponding to n^- is the smallest of all and is close to the value 0.56 from $\pi^- p$ experi-

ment at 20–360 GeV/c [16]. On the other hand, the presence of knocked out protons in a multiplicity tends to enhance the slope of the dependence D on $\langle n \rangle$.

Now, using this argument we can explain qualitatively the discrepancies in Figs. 1, 2. Namely, as it is known from nuclear emulsion data [17], the mean number of knocked out protons (“grey” tracks) does not depend on the primary energy, while the mean multiplicity of the relativistic particles (“shower” tracks) increases with the energy. Therefore, the relative amount of knocked out protons in the streamer chamber experiment at 200 GeV/c is less than that of ours and hence one can expect smaller slope of the corresponding line in the Fig. 1.

The result of the electronic experiment in Fig. 2 concerns the “shower” particles with $\beta \geq 0.85$ i.e. protons of momenta below ~ 1.5 GeV/c are fully excluded. In our experiment we subtract protons with momenta below ≈ 500 MeV/c which corresponds approximately to half of all knocked out protons (as it can be estimated from the ratio $\langle n_p \rangle / \langle Q \rangle$). Therefore our multiplicities in Fig. 2 contain a rather large amount of knocked out protons and hence the slope of our line is larger than that in experiment [12].

II. Scaling of the Multiplicity Distributions

Using the results of the previous section we can define scaling variables according to prescription (1). From relations (1), (2) it simply follows that the mean value and dispersion satisfy:

$$\langle z' \rangle = 1, \quad D_{z'} = \sqrt{\langle z'^2 \rangle - \langle z' \rangle^2} = a. \quad (5)$$

Therefore, in the case of our data, if we use the variable (2) with the corresponding parameters listed in Table 3 the resulting distributions up to the second moment will not depend on the target and projectile particle.

In Fig. 8 the scaling of the distribution $\psi(z')$ for negatively charged particles from $\bar{p}A$ collisions is demonstrated. Since our starting distributions $P(n^-)$ are not corrected with respect to secondary interactions, γ -conversions and decays within the target, uncorrected values $a_{uncorr} = 0.65$, $b_{uncorr} = -0.60$ have been used in the variable z' correspondingly. In the figure it is seen that within statistical errors a single curve can be drawn through all the distributions, none of them showing any systematic deviations.

In Fig. 9 we show the distribution $\psi(z')$ of the slow protons from $\bar{p}A$ interactions. Within statistical errors, the distributions can be as well described by a single curve for all nuclear targets.

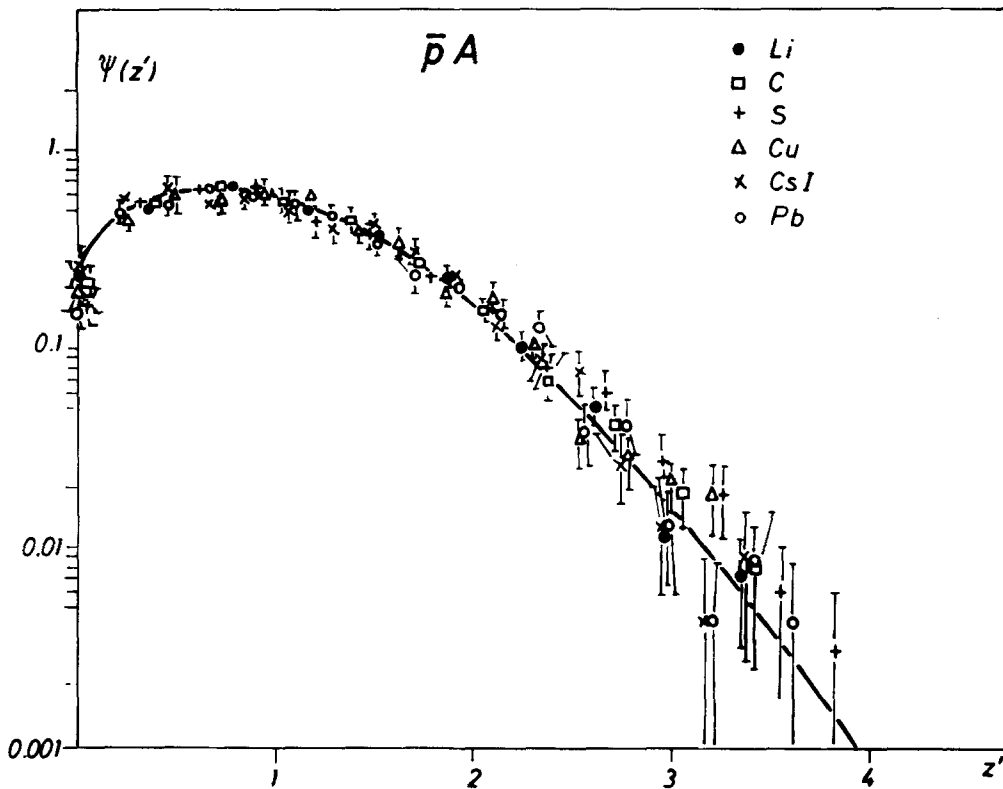


Fig. 8. Multiplicity distribution of negatively charged particles from $\bar{p}A$ interactions in terms of the modified scaling parameter z' . The curve corresponds to the parametrization described in the text, see (6a)

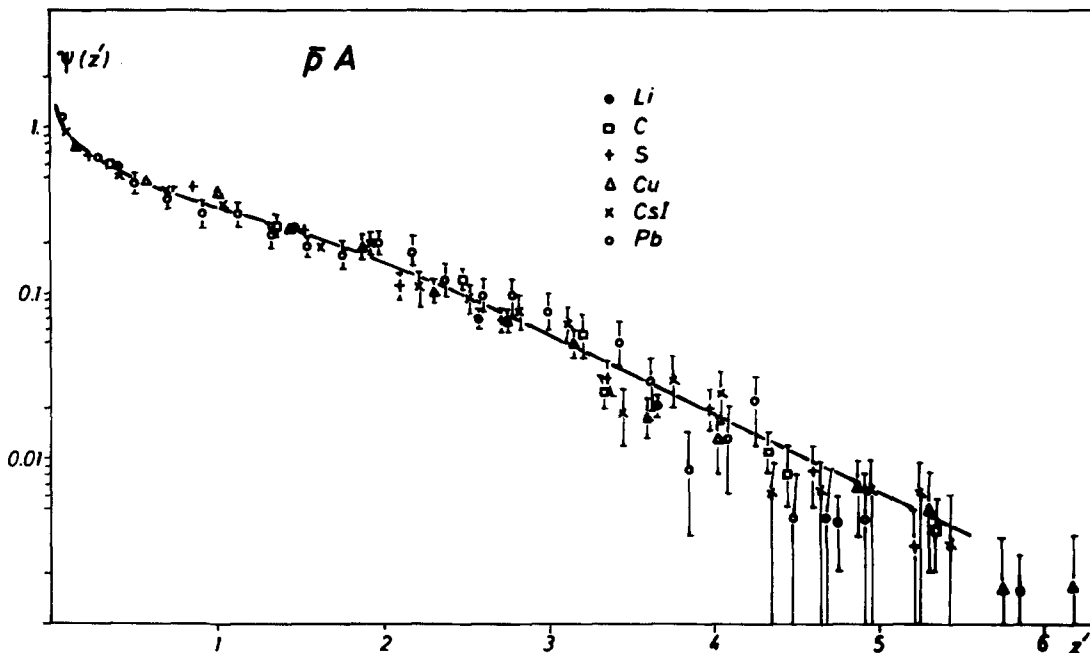


Fig. 9. Multiplicity distribution of identified protons in terms of modified scaling parameter z' . The curve corresponds to the parametrization described in the text, see (6b)

Using the scaling parameter (2) similar results can be obtained for all the other considered multiplicity distributions. There are no apparent differences between the distributions corresponding to the

primary particles π^- , K^- , \bar{p} in our event sample. Our present statistics is however rather low, especially that of π^-A , K^-A events. Hence for a description of the dependences in Figs. 8, 9, where all

the experimental distributions are normalized to unity, we made a fit which included the data from $\pi^- A$, $K^- A$, $\bar{p}A$ interactions together:

$$\psi_{n^-}(z') = (0.185 + 3.09 z' + 14.3 z'^3 + 5.10 z'^5 - 0.303 z'^7) e^{-3.66 z'}; \quad \chi^2/\text{NDF} = 203/217, \quad (6a)$$

$$\psi_{n_p}(z') = e^{F(z')}, \\ F(z') = 1.59 - (2.74 z' - 0.262 z'^2 + 0.230 z'^3 - 0.0204 z'^4) z'^{-0.777}; \quad \chi^2/\text{NDF} = 235/198. \quad (6b)$$

The results on $P(n^-)$ can also be analyzed using the ordinary KNO scaling variable $z = n/\langle n \rangle$ [10, 20]. In Fig. 10 there is shown the comparison of data on $\bar{p}A$ (all distributions normalized to unity) with our fit

$$\psi(z) = (1.85 z + 18.0 z^3 - 3.67 z^5 + 0.213 z^7) \cdot e^{-3.10 z}; \quad \chi^2/\text{NDF} = 258/218 \quad (7)$$

and with the empirical curve [11] proposed by Slattery ($\chi^2/\text{NDF} = 272/218$). It is seen that within statistical errors all distributions are consistent with both the curves, but the experimental distributions corresponding to the heavy nuclei seem to be slightly broader than that corresponding to light ones. This

spreading is a consequence of the choice $z = n/\langle n \rangle$ and the relation (2), giving

$$D_z = \sqrt{\langle z^2 \rangle - \langle z \rangle^2} \\ = \frac{1}{\langle n \rangle} \sqrt{\langle n^2 \rangle - \langle n \rangle^2} = a + \frac{b}{\langle n \rangle}. \quad (8)$$

Since the parameter b is negative, the dispersion increases with the mass of a target.

We conclude that the scaling variable z' is better for a unique description of the multiplicity distributions which fulfil the linear relation (2), than the usual $z = n/\langle n \rangle$. However, if we use the scaling variable z' , exact scaling requires all moments $C_K = \langle (n - \langle n \rangle)^K \rangle / D^K$ to be constant ($K=3$ corresponds to the skewness). In the Figs. 11, 12 we have shown the dependence of the third moment on the mass of the target. It is seen that in the case of n^- the dependence is nearly constant within statistical errors but the skewness corresponding to the distribution of n_p is apparently decreasing with the mass number A . One observes qualitatively the same dependence for higher moments also (not shown). It is seen that in the case of distributions of knocked out protons the scaling is only approximate.

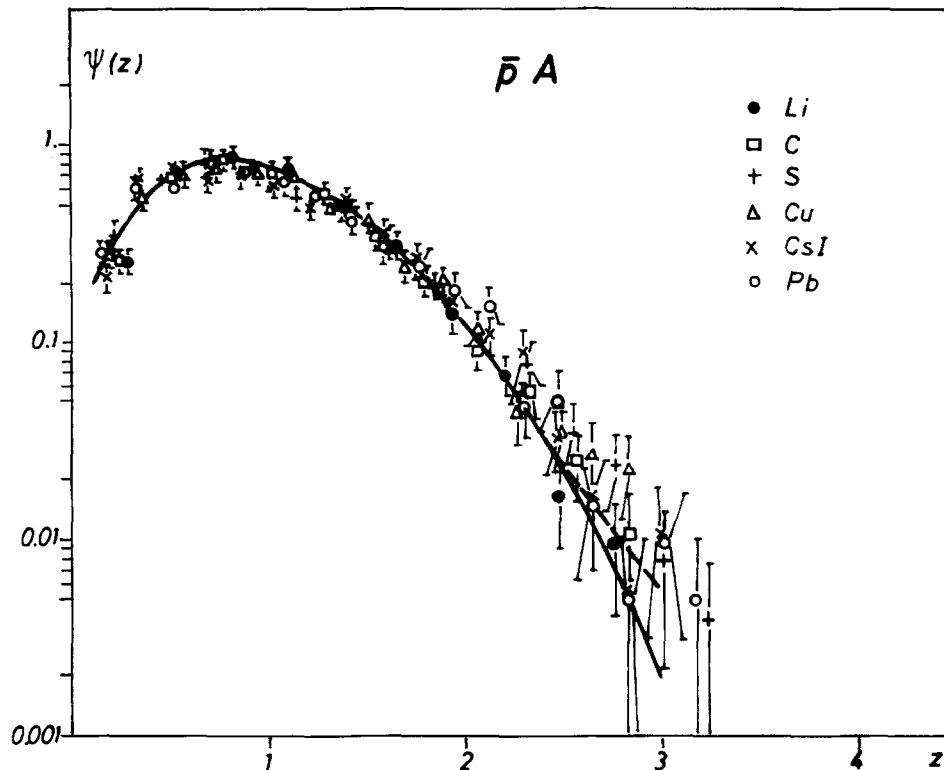


Fig. 10. Multiplicity distribution of negatively charged particles from $\bar{p}A$ interactions in terms of the usual scaling parameter $z = n/\langle n \rangle$. The solid line is Slattery's parametrization [11] from pp interactions, the dashed line corresponds to the parametrization described in the text, see (8)

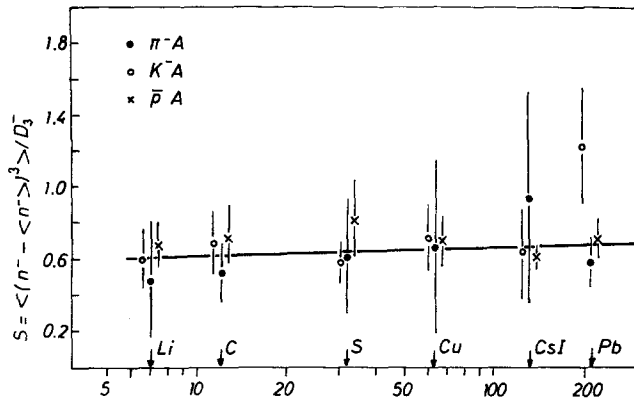


Fig. 11. The skewness of the multiplicity distribution of negatively charged particles as a function of mass number A . The straight line is the result of a linear fit

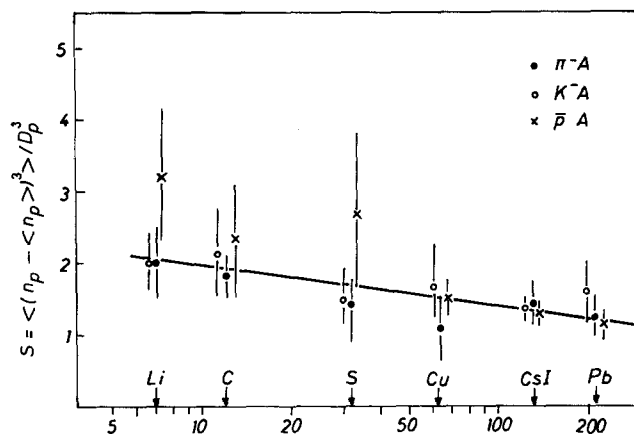


Fig. 12. The skewness of the multiplicity distribution of identified protons ($p_{LAB} \lesssim 500$ MeV/c) as a function of mass number A . The straight line is the result of a linear fit

Our results suggest an interpretation of multiplicity scaling in terms of stochastic-statistical models [18, 19]. Following these models, the shape of the scaling function depends on the dynamical process. Scaling itself, however, is due to general statistical laws, which can hold in a very similar way even for the production of particles of quite different origin as the knocked out protons and the particles resulting from the process of hadronization.

4. Conclusions

We have studied the multiplicity distributions of charged particles produced from π^- , K^- , and \bar{p} in-

teractions with the nuclei Li, C, S, Cu, CsI, Pb at 40 GeV/c obtained with the streamer chamber spectrometer RISK. The main results of this paper are the following:

1) It is shown that the linear dependence $D = a\langle n \rangle + b$ is satisfied for the multiplicity distribution of the secondary particles n_{ch} , n^+ , n^- , n_{FAST} , n_{FAST}^+ , n_p and the net charge Q also. Beside that, the parameters a and b within statistical errors, do not depend on the projectile particle.

2) The parameters a and b corresponding to the negatively charged particles are close to those from $\pi^- p$ interactions measured in the energy interval 20–360 GeV. Larger slopes of the other lines are explained as an effect of knocked out protons.

3) As a consequence of the linear dependence $D = a\langle n \rangle + b$ the scaling variable $z = n/\langle n \rangle$ is excluded for an exact uniform description of the multiplicity distributions for different nuclei and the variable $z' = (an + b)/(a\langle n \rangle + b)$ is preferred. If we use the scaling variable z' in any distribution, then within statistical errors a single curve can describe the distributions for different nuclei and primary particles.

References

1. Z. Koba, N.B. Nielsen, P. Olesen: Nucl. Phys. **B40**, 317 (1970)
2. W. Morse et al.: Phys. Rev. **D7**, 66 (1977); D. Brick et al.: Phys. Rev. **D25**, 2794 (1982); S. Barish et al.: Phys. Rev. **D9**, 2689 (1974); A. Firestone et al.: Phys. Rev. **D10**, 2080 (1974); J.L. Bailly et al.: CERN/EP 83-192
3. G.J. Alner: Phys. Lett. **138B**, 304 (1984)
4. A.J. Buras et al.: Phys. Lett. **47B**, 251 (1973)
5. N.S. Amaglobeli et al.: Yad. Fiz. **25**, 335 (1977)
6. A. Wroblewski: Acta Phys. Pol. **B4**, 857 (1973)
7. B.S. Yuldashev et al.: Acta Phys. Pol. **B9**, 513 (1978)
8. S.A. Azimov et al.: Nucl. Phys. **B107**, 45 (1976)
9. C. DeMarzo et al.: Phys. Rev. **D26**, 1019 (1982)
10. E.G. Boss et al.: Z. Phys. C - Particles and Fields **26**, 43 (1984)
11. P. Slattery: Phys. Rev. Lett. **29**, 1624 (1972)
12. J.E. Elias et al.: Phys. Rev. **D22**, 13 (1980)
13. G. Bohm et al.: Yad. Fiz. **35**, 700 (1982)
14. P. Závada: Ph.D. Thesis, Prague 1983
15. N.S. Angelov et al.: Yad. Fiz. **26**, 811 (1977)
16. E. Wolf et al.: Nucl. Phys. **B87**, 325 (1975)
17. K.B. Gulamov et al.: Physics of elementary particles and atomic nuclei. JINR-Dubna **3**, 554 (1978)
18. P. Carruthers, C.C. Shih: Phys. Lett. **127B**, 242 (1983)
19. P. Carruthers, C.C. Shih: Preprint LA-UR-84-250, Los Alamos
20. E.G. Boss et al.: Lett. Nuovo Cimento **41**, 209 (1984)